EUROTeV-Report-2008-xxx-1

# Review of the CLIC Energy Collimation System and Spoiler Heating

J. Resta-López *, L. Fernández-Hernando †

July 15, 2008

**Abstract**

Since the beam parameters of the Compact Linear Collider (CLIC) have recently been updated, one might wonder if considering the new beam parameters the energy collimator can withstand the direct impact of an entire bunch train. In this report we revisit the energy spoiler survival issue for CLIC. After describing the general features of the CLIC collimation system, we calculate the increment of temperature due to instantaneous energy deposition by a direct impact of a bunch train in the energy spoiler. The code FLUKA is used to simulate the energy deposition in three different spoiler designs. The suitability of using a beryllium based spoiler is also discussed.

*JAI, Oxford Univeristy, UK
†STFC/DL/ASTeC, Daresbury, Warrington, UK

# 1 Introduction

The Compact Linear Collider (CLIC), operating at beam energies of the order of TeV, will collide beams with transverse energy density of the order of $\mathrm{GJ/mm^2}$ ($\simeq 6.2 \times 10^{18}$ $\mathrm{GeV/mm^2}$), what means a very high damage potential of the beam. Therefore, protection is necessary against mis-steered or errant beams, which can hit and damage components of the machine. In CLIC a postlinac energy collimation system is dedicated to intercept these mis-steered beams. This collimation system consists of an absorber and an upstream thin spoiler or scraper, whose purpose is to increase the angular divergence of an incident beam. This increases the beam size at the downstream absorber and reduces thus the risk of material damage in the absorber.

The choice of the material to make the spoiler is determined by the electrical, thermal and mechanical properties of the material. A spoiler with high electrical conductivity is desired to reduce the wakefield effects and then to keep the beam stability. On the other hand, the thermal and mechanical properties define the robustness of the spoiler. Survival of the material is desired in case of impact of the full bunch train.

In the case of CLIC the limits of temperature rise due to the heat deposition by an entire train for spoiler survival were analytically computed in [1]. They considered transverse Gaussian bunches at the spoiler position and solved the time-dependent heat equation in two spacial dimensions near an interface with vacuum. According to this study, they concluded that a spoiler made of beryllium (Be) could survive the impact of a full train with charge $N_e = 4 \times 10^9$ electrons/positrons (bunch population) and 154 bunches per train. However, since 2005 the CLIC parameters have been updated and optimised (see [2] and [3]). Table 1 summarise the main parameters of CLIC for centre-of-mass energies 0.5 GeV and 3 TeV. The two first columns correspond to parameters set previous to the year 2005. The third column shows parameters set as of mid 2005 [2] and the fourth column as of mid 2007 [3].

Currently the train charge is almost two times higher than that used in Ref. [1]. Therefore, new calculations have to be done to study the survivability of the CLIC spoiler considering the most recent beam parameters (2007). In this report we revisit the spoiler survival issue. First, in Section 2 we describe briefly the CLIC collimation system. In Section 3 we review the characteristics and chromatic properties of the beam at the momentum spoiler position. In Section 4 we describe some important issues on spoiler heating and temperature increase due to the ionization energy deposition by direct beam impact on a thin spoiler. Finally we have also performed, by using the code FLUKA [4], some simulations of heat deposition by the bunch train passage in the spoiler. The simulation results are shown in Section 5, and possible composite and structural modifications for the improvement of the spoiler are discussed.

# 2 The CLIC Collimation System

The CLIC beam delivery system (BDS), downstream of the main linac, consists of a 460 m long final focus system (FFS) [5], and almost 2000 m long collimation system.

Table 1: Overall parameters of CLIC for centre-of-mass energies 0.5 TeV and 3 TeV.

| parameter | value | | | |
|---|---|---|---|---|
| Centre-of-mass energy (TeV) | **0.5 TeV** | **3 TeV** | **3 TeV** (2005) | **3 TeV** (2007) |
| Design luminosity ($10^{34}$ cm$^{-1}$s$^{-1}$) | 2.1 | 8.0 | 6.5 | 5.9 |
| Energy spread (%) | 1 | 1 | 1 | 1 |
| Photons/electron | 0.75 | 1.53 | 1.1 | 2.2 |
| Main linac RF frequency (GHz) | 30 | 30 | 30 | 11.994 |
| Linac repetition rate (Hz) | 200 | 100 | 150 | 50 |
| Particles/bunch at IP ($\times 10^9$) | 4.0 | 4.0 | 2.56 | 3.72 |
| Bunches/pulse | 154 | 154 | 220 | 312 |
| Bunch length ($\mu$m) | 35 | 35 | 30.8 | 45 |
| Bunch separation (ns) | 0.67 | 0.67 | 0.267 | 0.5 |
| Bunch train length ($\mu$s) | 0.102 | 0.102 | 0.0587 | 0.156 |
| Emittances $\gamma\epsilon_x/\gamma\epsilon_y$ ($10^{-8}$ rad·m) | 200/1 | 68/1 | 66/1 | 66/2 |
| Unloaded/loaded gradient (MV/m) | 172/150 | 172/150 | 172/150 | 120/100 |
| Beam power/beam (MW) | 4.9 | 14.8 | 20.3 | 14 |
| Total site AC power (MW) | 175 | 410 | 418 | 322 |
| Overall length (km) | 7.7 | 33.2 | 33.2 | 47.9 |

Recently, the CLIC BDS has been optimised and updated according the new beam parameters [6]. However, no significant changes have been done to the collimation section. The optics of the CLIC collimation system is shown in Fig. 1, where we can distinguish two sections:

- A 1375 m long section downstream of the main linac for *energy collimation*. This section fulfils an important protection function intercepting mis-steered beams, which may be produced by failure modes in the linac[1]. These failure modes determine the energy collimation depth. For CLIC a thin spoiler ($\sim$ 0.5 radiation length) made of beryllium, located at a position with non-zero horizontal dispersion ($D_x$ = 0.27 m), and a thick downstream absorber ($\sim$ 20 radiation length) are dedicated to protect against beams with off-energy of about $\pm$1.5 % of the nominal energy [7]. We have set the collimator aperture to intercept beam with energy deviation larger than 1.3 %.

  The purpose of the spoiler is to increase the phase space of the incident beam. In this way the scattered beam arrives to the downstream absorber with the transverse density reduced for passive protection of the absorber. In this scheme spoiler/absorber, the spoiler must handle high peak beam densities and generally passive protection of the spoiler is desired, i.e., the spoiler has to withstand the impact of as many bunches as possible. For this reason the design of the spoiler presents technically a challenge.

[1]Momentum errors in the main linac can be cause, e.g., if the beam is injected at the wrong phase or with the wrong charge, or due to a missing drive beam. This may generate errant beams which must be intercepted at the exit of the linac

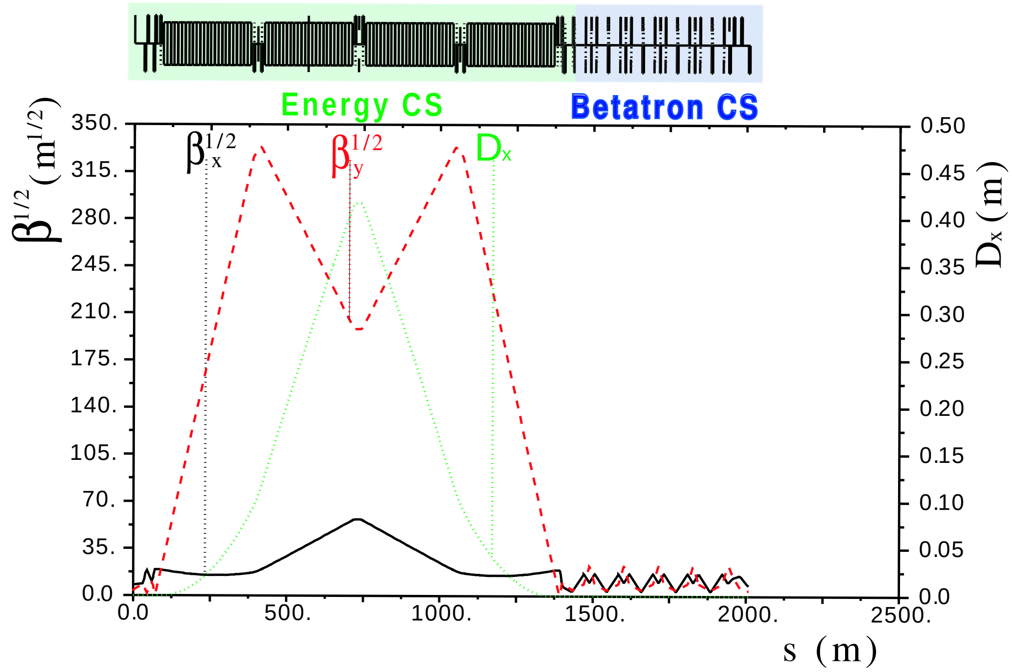


Figure 1: Horizontal dispersion and square root of the betatron functions for the CLIC baseline collimation system.

- Downstream of the energy collimation section, a dispersion-free section is dedicated to *betatron collimation*, i.e., to clean the transverse halo of the beam, reducing thus the experimental background in the interaction region. In total eight spoilers made of Be and and eight copper (Cu)-coated Titanium (Ti) absorbers are devoted to collimate the two transverse phases $x$–$x'$ and $y$–$y'$. In this case, the necessary collimation depths are determined from the conditions that beam particles and synchrotron radiation photons emitted in the final quadrupoles should not hit any magnet apertures on the incoming side of the interaction point. According to this criterium, for the case of CLIC with 3 TeV centre-of-mass energy, the collimation depths were estimated to be less than 14 $\sigma_x$ (horizontal plane) and 83 $\sigma_y$ (vertical plane) [8]. However, due to nonzero dispersion across the final doublet, the number for the horizontal beam size $\sigma_x$ includes both betatron and dispersive components, roughly equal in magnitude, such that the actual horizontal collimation depth at a place with zero dispersion needs to be $\sqrt{2}$ smaller, or about 10 $\sigma_x$. Due to recent changes in the vertical emittance (see Table 1) and the vertical beta function across the final doublet the initial vertical depth 83 $\sigma_y$ has been reduced to 44 $\sigma_y$ [9].

  Unlike the momentum spoiler, the spoilers in the betatron collimation section were designed to be sacrificial, i.e. they would certainly be destroyed if they suffer the direct impact of a bunch train (for example, if the momentum collimators are not set properly).

Table 2 summarises the CLIC post-linac collimator parameters. The horizontal aperture for the momentum collimator is set to $a_x = D_x \delta_{\text{aper}}$, with the energy offset $\delta_{\text{aper}} = \pm 1.3$ %.

Table 2: CLIC post-linac collimator parameters. Longitudinal position, horizontal and vertical $\beta$-functions, horizontal dispersion, horizontal and vertical half gaps, geometry of the collimator and material.

| s[m] | Name | $\beta_x$[m] | $\beta_y$[m] | $D_x$[m] | $a_x$[mm] | $a_y$[mm] | Geometry | Material |
|---|---|---|---|---|---|---|---|---|
| 566.502 | ENGYSP | 1406.33 | 70681.9 | 0.27 | 3.51 | 25.4 | rect | Be |
| 731.502 | ENGYAB | 3213.03 | 39271.5 | 0.417 | 5.41 | 25.4 | rect | Ti(Cu coated) |
| 1490.28 | YSP1 | 114.054 | 483.253 | 0. | 10. | 0.08 | rect | Be |
| 1506.1 | XSP1 | 270.003 | 101.347 | 0. | 0.08 | 10. | rect | Be |
| 1583.3 | XAB1 | 270.102 | 80.9043 | 0. | 1. | 1. | ellip | Ti(Cu coated) |
| 1601.12 | YAB1 | 114.054 | 483.184 | 0. | 1. | 1. | ellip | Ti(Cu coated) |
| 1603.12 | YSP2 | 114.054 | 483.188 | 0. | 10. | 0.08 | rect | Be |
| 1618.94 | XSP2 | 270.002 | 101.361 | 0. | 0.08 | 10. | rect | Be |
| 1696.14 | XAB2 | 270.105 | 80.9448 | 0. | 1. | 1. | ellip | Ti(Cu coated) |
| 1713.96 | YAB2 | 114.055 | 483.257 | 0. | 1. | 1. | ellip | Ti(Cu coated) |
| 1715.96 | YSP3 | 114.054 | 483.253 | 0. | 10. | 0.08 | rect | Be |
| 1731.78 | XSP3 | 270.003 | 101.347 | 0. | 0.08 | 10. | rect | Be |
| 1808.98 | XAB3 | 270.102 | 80.9043 | 0. | 1. | 1. | ellip | Ti(Cu coated) |
| 1826.8 | YAB3 | 114.054 | 483.184 | 0. | 1. | 1. | ellip | Ti(Cu coated) |
| 1828.8 | YSP4 | 114.054 | 483.188 | 0. | 10. | 0.08 | rect | Be |
| 1844.63 | XSP4 | 270.002 | 101.361 | 0. | 0.08 | 10. | rect | Be |
| 1921.83 | XAB4 | 270.105 | 80.9448 | 0. | 1. | 1. | ellip | Ti(Cu coated) |
| 1939.65 | YAB4 | 114.055 | 483.257 | 0. | 1. | 1. | ellip | Ti(Cu coated) |

Geometrical parameters of the CLIC energy spoiler and absorber are shown in Table 3 following the notation of Fig. 2. Generally a tapered geometry is used in order to reduce the geometrical wakefield effects. The spoilers are designed with transverse rectangular cross view and $L_F = 0$ (or flat part length very small compared with that for the absorber), while the absorbers were designed with elliptical transverse geometry.

Table 3: Geometrical parameters of the CLIC energy spoiler and absorber.

| Parameter | **spoiler ENGYSP** | **absorber ENGYAB** |
|---|---|---|
| Vertical half-gap $h$ [mm] | 25.4 | 25.4 |
| Horizontal half-gap $a$ [mm] | 3.51 | 5.4 |
| Tapered part radius $b$ [mm] | 6.21 | 6.21 |
| Tapered part length $L_{\text{T}}$ [mm] | 90.0 | 27 |
| Taper angle $\theta_{\text{T}}$ [rad] | 0.03 | 0.03 |
| Flat part length $L_{\text{F}}$ [mm] | 0.0 | 646 |

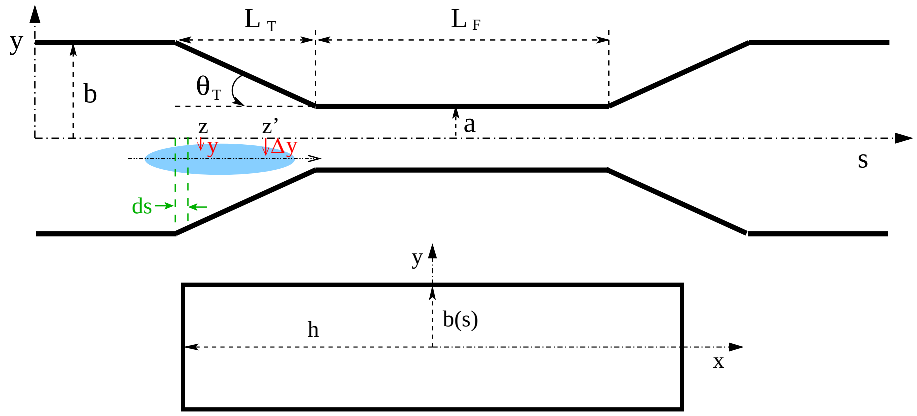


Figure 2: Top: longitudinal view of a tapered collimator. An oncoming particle bunch is schematically represented by the solid ellipse. Bottom: cross-sectional view in the case of a rectangular collimator.

# 3 Transverse Density of the Beam at the Energy Spoiler

In order to study the characteristics of the beam at the spoiler position, we have performed multiparticle tracking simulations using the code MAD [10]. A transverse Gaussian distribution of 10000 macroparticles is tracked from the start of the CLIC BDS to the energy spoiler ENGYSP. We have studied two cases: one using a monochromatic beam with 1.5 % energy offset from the the nominal beam energy 1.5 TeV, and another using a beam with 1.5 % centroid energy offset and an uniform energy distribution with 1 % full width energy spread.

Figure 3 shows the horizontal particle density at spoiler position for both cases. Using a realistic beam particle distribution with an uniform energy spectrum of 1 % full energy spread, the density of the distribution is reduced by a factor 50 with respect to the density peak of the monochromatic distribution. Figures 4 and 5 shows the corresponding particle distribution projected on the vertical plane and the energy spectrum, respectively. For an uniform energy distribution (with 1 % energy spread), the energy density is about 450 times smaller than the energy density peak of the monochromatic distribution.

More details of the characteristics and chromatic behaviour of the beam at the spoiler are shown in Figures 6 and 7 for several centroid energy offsets $\delta_0$. On one hand, Figure 6 shows the particle density in the plane $x$–$y$, normalised to the number of particles per bunch, for two different monochromatic Gaussian beams with $\delta_0 = 1.25$ % and $\delta_0 = 1.5$ %. When $\delta_0 = 1.5$ % the entire beam impacts on the jaw of the spoiler. On the other hand, Figure 7 shows an example of a transverse density distribution considering a beam with an uniform energy spectrum with a full width energy spread of 1 %. In this case we have compared $\delta_0 = 0$ %, $\delta_0 = 1.5$ % and $\delta_0 = 3$ %. For the sake of benchmarking, it is worth mentioning that, in the same conditions, tracking simulations using the code PLACET [11] have given similar results.

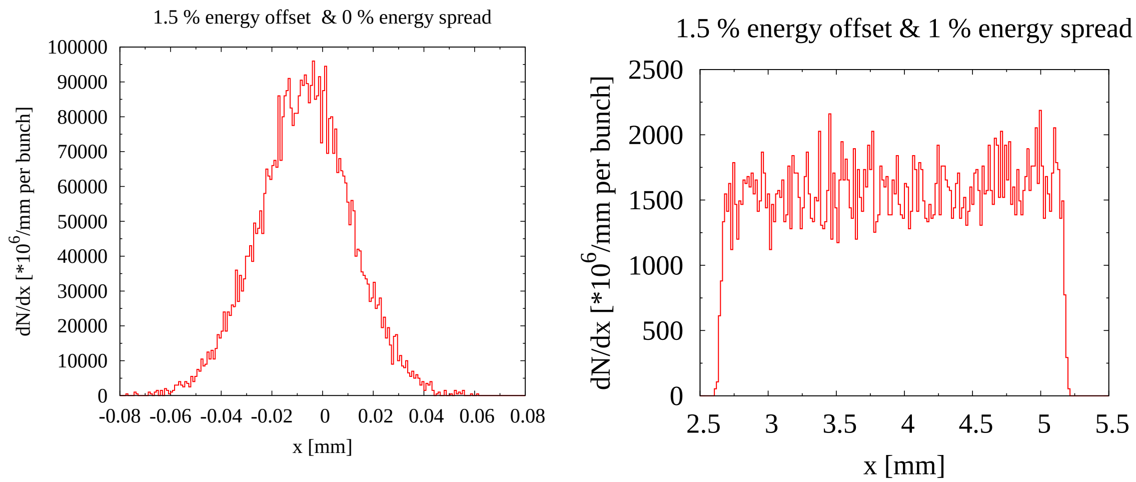


Figure 3: Left: horizontal particle density at spoiler position for a distribution with 1.5 % mean energy offset and no energy spread. Right: horizontal particle density at spoiler position for a distribution with 1.5 % mean energy offset and 1 % full width energy spread.

The horizontal beam size at the spoiler position with first order dispersion $D_x$ can be calculated from $\sigma_x = \sqrt{D_x^2(\langle\delta^2\rangle - \langle\delta\rangle^2) + \beta_x\epsilon_x}$, where $\delta = \Delta E/E_0$ indicates the energy deviation and the brackets $\langle\ldots\rangle$ the average over the energy distribution. For a Gaussian energy distribution with a centroid energy offset $\delta_0$ and a width energy spread $\sigma_E$ one obtains: $\langle\delta^2\rangle = \sigma_E^2 + \delta_0^2$ and $\langle\delta\rangle = \delta_0$. Therefore, for a Gaussian energy distribution, using the CLIC parameters and $\sigma_E = 1$ %, one obtains $\sigma_x = \sqrt{D_x^2\sigma_E^2 + \beta_x\epsilon_x} \simeq 796$ $\mu$m at the momentum spoiler.
If now we assume an uniform flat energy distribution with a full width energy spread $\sigma_E$ and a mean energy offset $\delta_0$, we obtain: $\langle\delta^2\rangle = \sigma_E^2/12 + \delta_0^2$ and $\langle\delta\rangle = \delta_0$. Therefore, $\sigma_x = \sqrt{D_x^2\sigma_E^2/12 + \beta_x\epsilon_x} \simeq 779.6$ $\mu$m at the momentum spoiler.
From the above results we can conclude that the transverse density of the beam at the spoiler depends significantly on the chromatic properties of the beam. Therefore, in the simulations the chosen initial energy spectrum (Gaussian or uniform shape and the energy spread) will be crucial for the estimation of the energy deposition in the spoiler and the subsequent temperature rise. For instance, calculations performed assuming monochromatic Gaussian beams will give more pessimistic results (an upper limit to the temperature rise) than assuming a certain energy spread.

# 4 Temperature Increase Due to Energy Deposition by Direct Beam-Matter Interaction

The principal mechanism for spoiler/collimator damage is the instantaneous heat deposition. The main sources for such a heating are the energy deposition by direct beam-

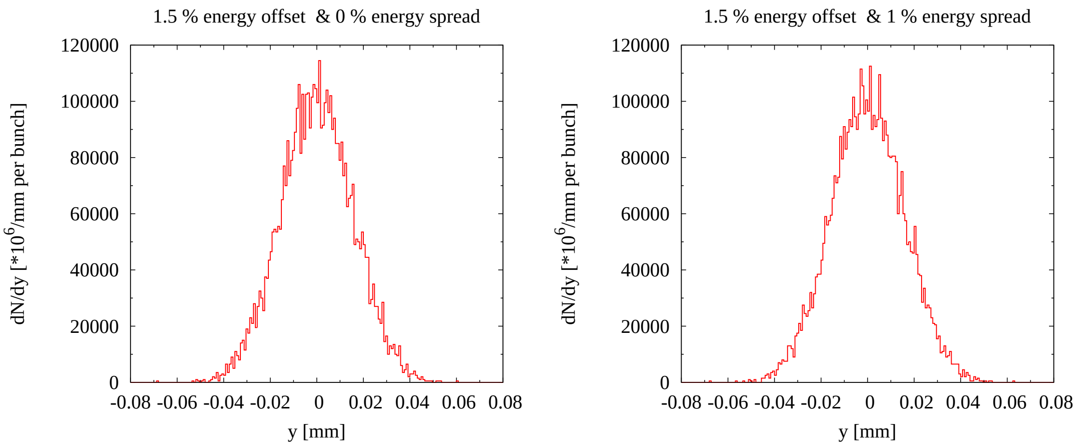


Figure 4: Left: vertical particle density at spoiler position for a distribution with 1.5 % mean energy offset and no energy spread. Right: vertical particle density at spoiler position for a distribution with 1.5 % mean energy offset and 1 % full width energy spread.

spoiler interaction, the image current heat deposition and the electric field breakdown. In this Section we study the most critical case, which is the instantaneous temperature rise of the spoiler due to a deep beam impact on the collimator. Mis-steered beams with energy offset $\gtrsim 1.3$ % of the nominal energy hit the spoiler. Since the thickness of the spoiler ENGYSP is significantly small in terms of radiation length[2] (0.25 $X_0$ or 0.5 $X_0$ at the base of the collimator), the electrons/positrons deposit energy basically by ionization, and practically no electromagnetic showers are developed. In this case, the instantaneous temperature rise is given by

$$\Delta T_{inst}(x, y, t = 0) = \frac{1}{\varrho C} \left( \frac{dE}{dz} \right) \rho(x, y) \ , \tag{1}$$

where $\varrho$ is the density of the spoiler material, $C$ the heat capacity and $\rho(x, y)$ is an arbitrary transverse beam density. The energy deposition per unit of length is denoted as $(dE/dz)$, whose value can be determined from the Bethe-Bloch formula [12]. Table 4 shows some properties for several materials, including the radiation length and the minimum energy deposition for ionization.

If we assume a Gaussian beam with horizontal and vertical rms sizes $\sigma_x$ and $\sigma_y$, respectively, at the spoiler position, then the peak of instantaneous temperature rise by the impact of a full bunch train is given by

[2]The radiation length, generally denoted as $X_0$, is defined as the mean distance over which a high energy electron loses all but $1/e$ of its energy by bremsstrahlung. The radiation length depends mostly on the atomic (or molecular) number $Z$ and weight $A$ of the material as [12]:

$$X_0 \simeq \frac{716.4 \text{ g} \cdot \text{cm}^{-2} A}{Z(Z+1) \ln(287/\sqrt{Z})} \ .$$

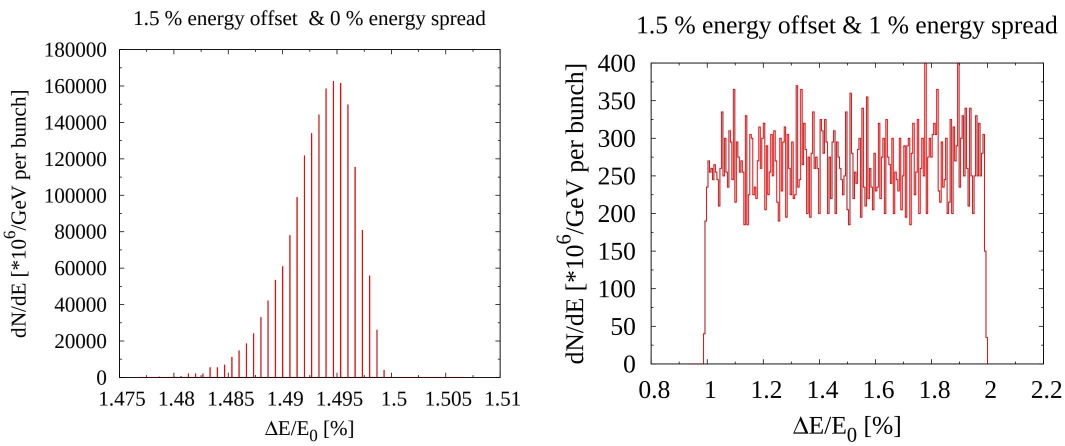


Figure 5: Left: energy density at spoiler position for a distribution with 1.5 % mean energy offset and no energy spread. Right: energy density at spoiler position for a distribution with 1.5 % mean energy offset and 1 % full width energy spread.

Table 4: Table of material properties at room temperature: $\varrho$ is the material density, $C$ the specific heat, $K$ the thermal conductivity, $\sigma$ the electrical conductivity, $X_0$ the radiation length, and $X_0 \cdot (dE/dz)_{\rm min}$ [MeV] is the minimum energy deposition for ionization per radiation length. Data obtained from [12, 13, 14, 15].

| **Material** | $\varrho$ [gm$^{-3}$] | $C$ [Jg$^{-1}$K$^{-1}$] | $K$ [Wm$^{-1}$K$^{-1}$] | $\sigma$ [$\Omega^{-1}$m$^{-1}$] | $X_0$ [m] | $X_0 \cdot (dE/dz)_{\rm min}$ [MeV] |
|---|---|---|---|---|---|---|
| Be | $1.84 \times 10^6$ | 1.825 | 200 | $1.67 \times 10^7$ | 0.353 | 103.98 |
| C | $2.26 \times 10^6$ | 0.709 | 119-165 | $7.27 \times 10^4$ | 0.188 | 74.38 |
| Ti | $4.54 \times 10^6$ | 0.523 | 30.7 | $2.0 \times 10^6$ | 0.036 | 23.87 |
| Cu | $8.96 \times 10^6$ | 0.385 | 401 | $6.0 \times 10^7$ | 0.014 | 18.04 |
| W | $19.3 \times 10^6$ | 0.132 | 173 | $1.81 \times 10^7$ | 0.0035 | 7.74 |

$$\Delta \hat{T}_{inst} = \frac{1}{\varrho C} \left( \frac{dE}{dz} \right) \frac{N_e N_b e}{2\pi \sigma_x \sigma_y} \ , \qquad (2)$$

where we have assumed a train with $N_b$ bunches, each of them containing $N_e$ electrons. However, for beams with a energy spread of $\sim 1$ % multiparticle tracking simulations using the codes MAD and PLACET (see Section 3) have shown that the transverse spot size of the CLIC beam is far from the Gaussian shape at the spoiler position and, in general, we have to consider the amplitude peak of an arbitrary transverse beam distribution $\rho(x, y)$ at the spoiler position.
During the impact of a full bunch train, the passage of a bunch through the spoiler occurs at a repetition frequency of 2 GHz (taking the bunch separation $t_b = 0.5$ ns corresponding to the CLIC parameters 2007). In order to determine the time evolution

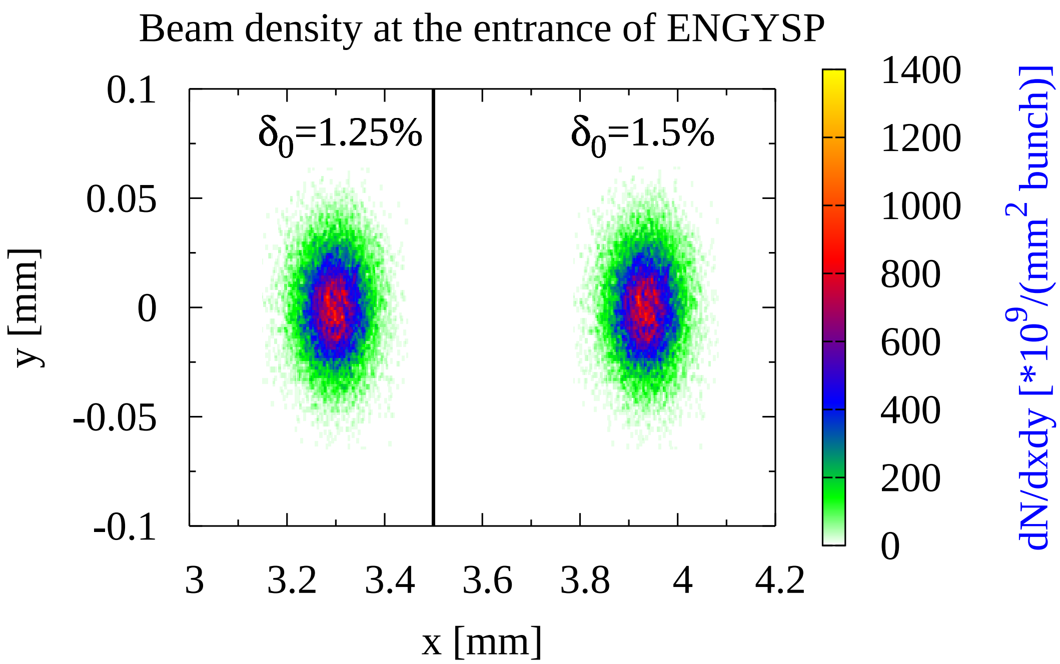


Figure 6: Transverse energy density at the CLIC energy spoiler position, from tracking of two transverse Gaussian distributions of 10000 macroparticles with centroid energy offsets $\delta_0 = 1.25$ % and $\delta_0 = 1.5$ %, and no energy spread. The result is normalised to $3.72 \times 10^9$ particles per bunch. The black line indicates the spoiler aperture.

of the temperature in the spoiler, it is necessary to solve the heat equation with a periodic excitation:

$$\frac{\partial T}{\partial t} = \frac{K}{\varrho C}\nabla^2 T + \sum_{n=0}^{N_b-1} \frac{\Delta T_{inst}}{t_b N_b}\delta(t - nt_b) \ . \tag{3}$$

The first term on the right hand side of Eq. (3) represents the heat conductivity, and the second term, containing the Dirac delta function $\delta(t - nt_b)$, takes into account the periodic heating bunch after bunch in the train. $\Delta T_{inst}$ can be obtained from Eq. (2). Possible cooling mechanisms, e.g. radiation cooling, can also contribute to the heat equation. At very high temperatures cooling by thermal radiation (black body radiation) becomes important. The radiated power per transverse area is given by:

$$h = \varepsilon \sigma_{\mathrm{SB}} T^4 \ , \tag{4}$$

where $\varepsilon$ is the emissivity of the material and $\sigma_{\mathrm{SB}} = 5.67 \times 10^{-8}$ $\mathrm{Wm^{-2}K^{-4}}$ the

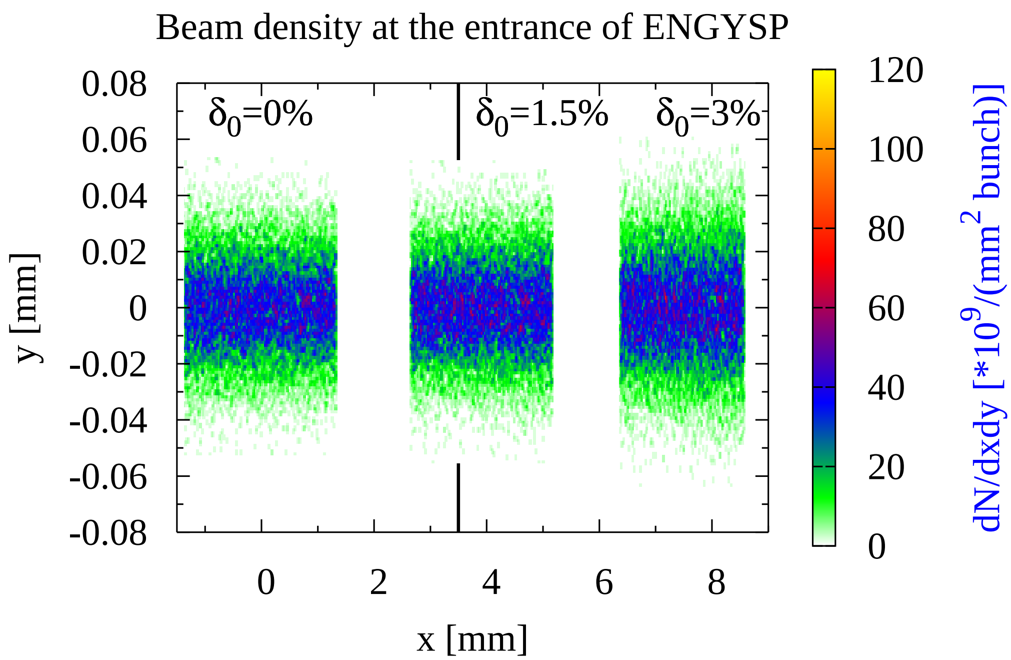


Figure 7: Transverse energy density at the CLIC energy spoiler position, from tracking of two transverse Gaussian distributions of 10000 macroparticles with mean energy offsets $\delta_0 = 0$ %, $\delta_0 = 1.5$ % and $\delta_0 = 3$ %, and with an uniform energy spectrum of 1 % full width spread. The result is normalised to $3.72 \times 10^9$ particles per bunch. The black line indicates the spoiler aperture.

Stefan-Boltzmann constant. If we take into account this cooling mechanism, a term $-2\varepsilon\sigma_{\rm SB}T^4 K/(\varrho C)$ has to be added to the right hand side of Eq. (3). Here we will neglect the contribution of the thermal radiation energy versus the energy deposited by ionization. Indeed, the ionization energy deposited during the passage of a train, crossing a length $L$ of spoiler material can be calculated from

$$E_{\rm ion} = N_b N_e L \frac{dE}{dz} \ . \tag{5}$$

Taking into account that the duration of a CLIC train is $N_b t_b$, the corresponding energy emitted by thermal radiation (black body) writes

$$E_{\rm black} = N_b t_b S \sigma_{\rm SB} T^4 \ , \tag{6}$$

where the emission surface is given by $S = 2\sigma_x L$. Let us consider, for example, a spoiler with length $L = 0.5$ X$_0$ made of Be, and the following beam parameters: $\sigma_x = 796$ $\mu$m, $N_b = 312$ bunches, $N_e = 3.72 \times 10^9$ electrons/positrons per bunch and $t_b = 0.5$ ns.

Considering also the upper temperature limit $T_{\text{melt}} \simeq 1560$ K and $(dE/dz)_{\text{min}}$ from Table 4, one obtains a ratio $E_{\text{black}}/E_{\text{ion}} \simeq 1.5 \times 10^{-6}$.

## 4.1 Limit for Instantaneous Temperature Rise of a Spoiler/Collimator

For the spoiler survival, the increment of temperature in the spoiler material must be lower than the *melting temperature* point, which we denote as $T_{\text{melt}}$. In principle, we do not take into account any cooling mechanism for the collimators. Therefore, assuming that the spoiler is operating at room temperature $T_{\text{room}} = 293$ K, the melting temperature excursion limit is given by $\Delta T_{\text{melt}} = T_{\text{melt}} - T_{\text{room}}$.
On the other hand, the rapid heating of the material caused by the impact of the train in the spoiler may contribute to the fracture of the material by *thermal stress*. Therefore, in order to evaluate the robustness of the material, it is also necessary to take into account the cyclic thermal stress, which is defined by the following equation:

$$\sigma_{cyc} \simeq \frac{1}{2}\alpha_T Y \Delta\hat{T}_{inst} \ , \tag{7}$$

where $\alpha_T$ is the thermal expansion coefficient, $Y$ is the elastic modulus (or Young modulus), and $\Delta\hat{T}_{inst}$ the instantaneous temperature rise obtained from Eq. (2).
The limit of thermal fracture is determined by the so-called ultimate tensile strength ($\sigma_{\text{UTS}}$), which is the maximum stress that the material can withstand. The ultimate tensile strength is related to the instantaneous temperature rise ($\Delta T_{\text{fr}}$) which causes mechanical fracture:

$$\sigma_{\text{UTS}} \simeq \frac{1}{2}\alpha_T Y \Delta T_{\text{fr}} \ . \tag{8}$$

The safe limit is usually chosen as $\Delta T_{\text{limit}} = \min[\Delta T_{\text{melt}}, \Delta T_{\text{fr}}]$. Generally the minimum corresponds to $\Delta T_{\text{fr}}$. The temperature rise limits $\Delta T_{\text{melt}}$ and $\Delta T_{\text{fr}}$ are registered in Table 5 for several materials, together with other material properties [13, 16].

# 5 Simulation Results

In order to estimate the energy density deposited and the corresponding instantaneous increase of temperature in the energy spoiler (ENGYSP) by the impact of an entire train, the code FLUKA [4] is used. The input is a train with 312 bunches, $3.72 \times 10^9$ particles per bunch, a beam energy of 1.5 TeV, and beam sizes at spoiler $\sigma_x = 796$ $\mu$m and $\sigma_y = 21.9$ $\mu$m. No energy spread has been considered. Furthermore, we have assumed that the beam is colliding 2 mm deep from the top of the spoiler and the energy is instantaneously deposited. It is also important to mention that in these simulations we do not take into account any bunch-to-bunch jitter, and all bunches of the train impact exactly on the same point of the spoiler surface.
Different configurations in terms of geometry and material composition for the spoiler design have been studied:

Table 5: The melting point temperature $T_{\rm melt}$, the melting temperature excursion limit $\Delta T_{\rm melt} = T_{\rm melt} - 293$ K, the thermal fracture temperature excursion limit $\Delta T_{\rm fr}$ (corresponding to the ultimate tensile strength from Eq. (8)), the elastic modulus $Y$, the coefficient of thermal expansion $\alpha_T$ and the ultimate tensile strength $\sigma_{\rm UTS}$, for the following materials: beryllium (Be), graphite (C), titanium (Ti), titanium alloy (90 % Ti, 6 % Al, 4% V), copper (Cu) and tungsten (W). For Ti alloy we have assumed the same melting point as for pure Ti. Data obtained from [13, 16].

| **Material** | $T_{\rm melt}$ [K] | $\Delta T_{\rm melt}$ [K] | $\Delta T_{\rm fr}$ [K] | $Y$ [$10^5$ MPa] | $\alpha_T$ [$10^{-6}$ K$^{-1}$] | $\sigma_{\rm UTS}$ [MPa] |
|---|---|---|---|---|---|---|
| Be | 1560 | 1267 | 370 | 2.87 | 11.3 | 600 |
| C | 3800 | 3507 | 14207 | 0.12 | 7.1 | 580 |
| Ti (pure) | 1941 | 1648 | 742 | 1.16 | 8.6 | 370 |
| Ti alloy | 1941(?) | 1648(?) | 1710 | 1.14 | 9.2 | 897 |
| Cu | 1358 | 1065 | 201 | 1.3 | 16.5 | 216 |
| W | 3695 | 3402 | 670 | 4.11 | 4.5 | 620 |

## 5.1 Spoiler made of beryllium, without flat part

Here we consider the nominal Be spoiler with the geometry shown in Fig. 8. It has been designed without flat part ($L_{\rm F} = 0$) in order to reduce the resistive wakefield effects. The total length of the spoiler is 0.5 $X_0$. To reduce the geometric wakefield effects the taper has a smooth transition angle ($\theta_{\rm T} = 0.03$ rad) between the aperture of the beam pipe to the narrowest gap of the spoiler jaws.

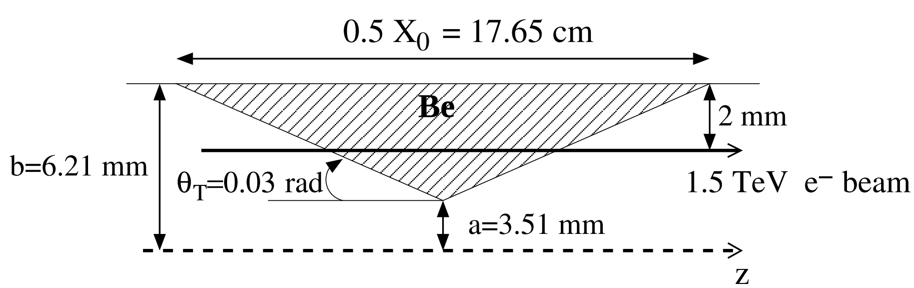


Figure 8: Schematic of the geometry used for the simulation using a Be spoiler. The figure is not to scale and the taper angle has been exaggerated.

Fig. 9 shows the energy density instantaneously deposited in the spoiler by the CLIC beam as calculated by the code FLUKA. The result is normalised per incident particle. The corresponding instantaneous temperature rise through the spoiler is shown in Fig 10. The maximum increment of temperature is of about 280 K, which is below of the melting limit ($\Delta T_{\rm melt} \simeq 1267$ K) and even below of the thermal fracture limit ($T_{\rm fr} \simeq 370$ K). Therefore this Be spoiler can withstand the impact of the full beam.
If the beam is colliding, for example, 2 mm deep from the top of the spoiler jaw, then

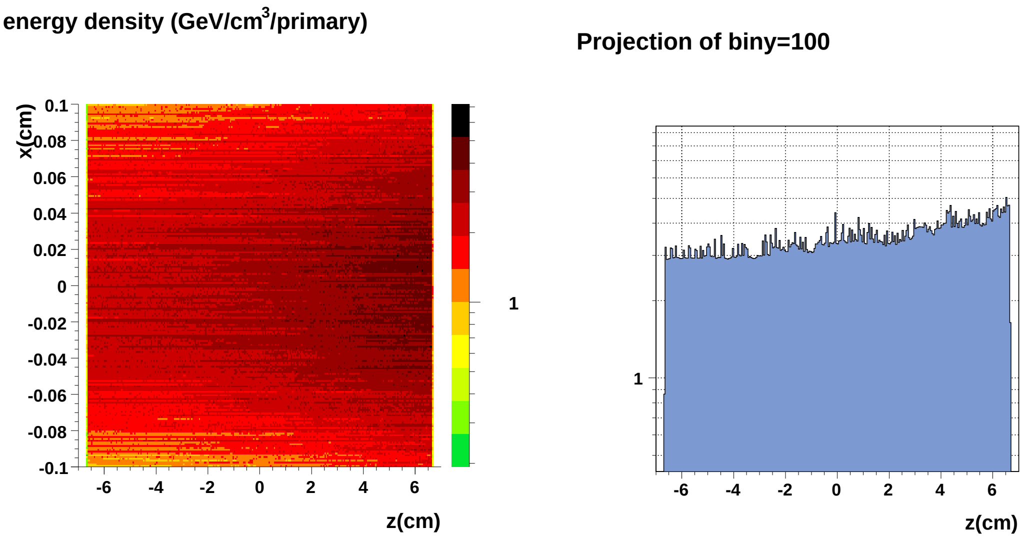


Figure 9: Density of energy deposited by ionization in the Be spoiler due to the impact of a 1.5 TeV $e^-$ beam. Right: projection of the energy density on the longitudinal coordinate $z$ for the slice $x = 0$ cm.

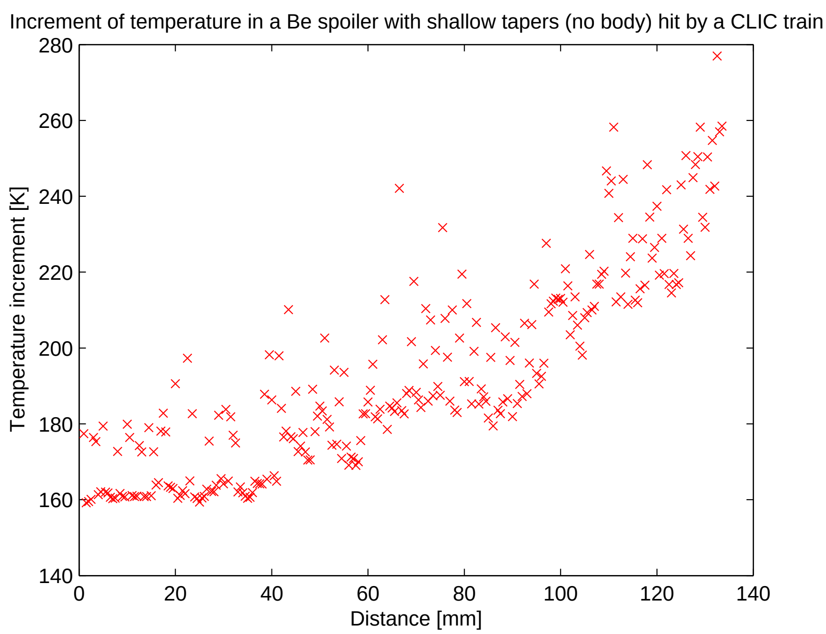


Figure 10: Instantaneous increment of temperature in a Be spoiler with shallow tapers and $L_{\mathrm{F}} = 0$ by the impact of an entire bunch train in CLIC.

the beam traverses about 4.7 cm of material (or 0.13 $X_0$ of Be). The radiation length for

the Be is large compared with other materials (see Table 4), and a distance of 0.13 $X_0$ in Be may be insufficient to disperse the beam by multiple Coulomb scattering up to safe transverse dimensions for passive protection of the downstream absorber.
To guarantee a minimum 0.5 $X_0$ for all depths of the beam-spoiler impact, we can modify the design above including a flat part of 0.5 $X_0$ ($L_F$ = 17.65 cm). Keeping the same structure for the tapers, the total length of the collimator would be then $2L_F + L_T$ = 35.3 cm. Apart from getting a longer spoiler, this new structure would further increase the wakefield effects respect to the spoiler without flat part.
For the sake of comparison, it is worth mentioning that for the International Linear Collider (ILC) spoilers [17], several spoiler options which combine different metals and graphite were tested with the aim to find a balance between short spoilers ($\sim$ 10 cm), that do not take up large amounts of space along the beamline, and low wakefield components, while ensuring appropriately lowered energy density incident on the downstream absorbers. Following a similar procedure, we can also try to study different options combining different metals for the CLIC momentum spoiler.

## 5.2 Spoiler with beryllium tapers and titanium alloy body

Let us add a bulk of Ti alloy (90 % Ti, 6 % Al, 4 % V) of 0.5 $X_0$ in the flat part of the spoiler, with tapers made of Be, such as shown in Fig. 11. Although the Ti has a higher melting and thermal fracture points than the Be, it has a lower radiation length than the Be, which results in a higher energy density deposition and, consequently, in a higher instantaneous temperature growth. Figure 12 shows the instantaneous energy deposition by ionization through the spoiler. The maximum deposition is registered in the Ti alloy body.
Concerning the wakefield issue, the electrical conductivity of the Ti ($\sigma = 2.0\times10^6\ \Omega^{-1}\mathrm{m}^{-1}$) is almost one order of magnitude smaller than the one of the Be ($\sigma = 1.67\times10^7\ \Omega^{-1}\mathrm{m}^{-1}$), increasing thus the wakefield effects.

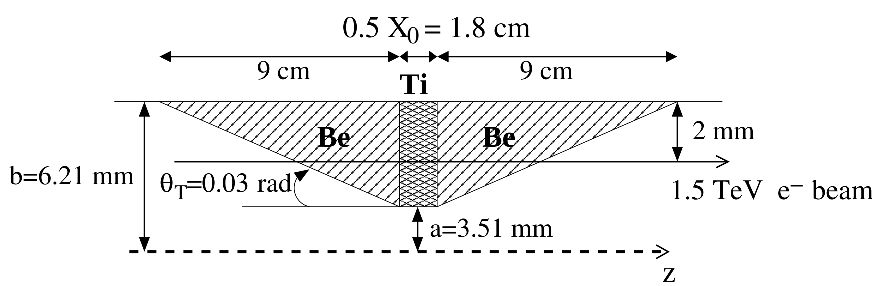


Figure 11: Schematic of the geometry used for the simulation using a Be + Ti alloy spoiler. The figure is not to scale and the taper angle has been exaggerated.

The instantaneous temperature rise in the spoiler is shown in Fig 13. We have found a maximum increment of temperature of about 1600 K, produced by the energy deposition in the additional body made of Ti. In this case the temperature rise is slightly below the

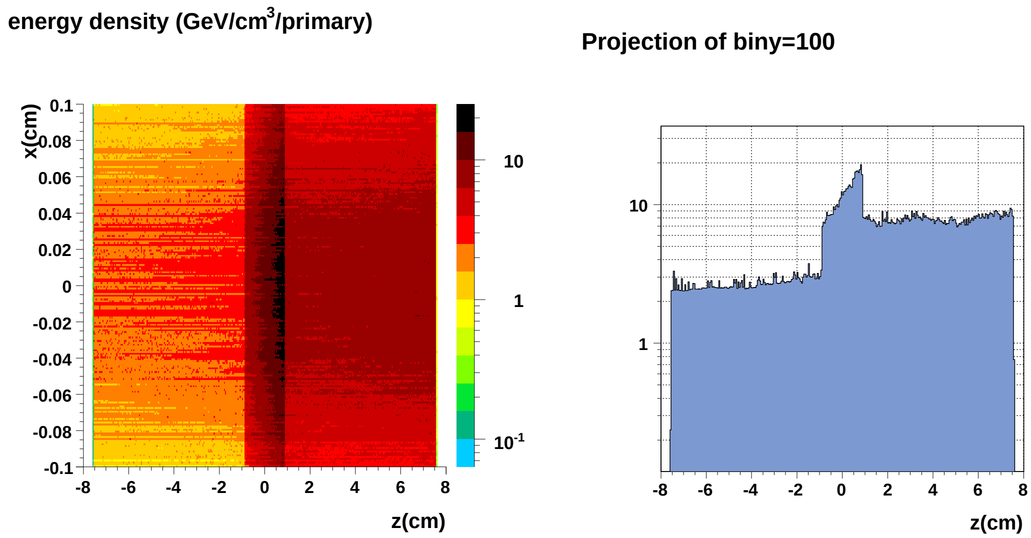


Figure 12: Density of energy deposited by ionization in the Be + Ti alloy spoiler due to the impact of a 1.5 TeV $e^-$ beam. Right: projection of the energy density on the longitudinal coordinate $z$ for the slice $x = 0$ cm.

allowed temperature excursion limit for the melting of the material ($\Delta T_{\mathrm{melt}} \simeq 1648$ K) and also below the thermal fracture limit ($\Delta T_{\mathrm{fr}} \simeq 1710$ K). The advantage of using Ti alloy (90 % Ti, 6 % Al, 4 % V) instead of pure Ti is its higher fracture toughness. Assuming a similar energy deposition in a bulk of pure Ti, the thermal fracture point ($\Delta T_{\mathrm{fr}} = 742$ K) would largely be surpassed.

## 5.3 Spoiler with beryllium tapers and copper body

We can also test another configuration with tapers made of Be and an additional body made of Cu for the flat part, as indicated in Figure 14. Due to the high electrical conductivity of the Cu (almost one order of magnitude higher than that for Ti) this design is advantageous in terms of decreasing wakefields. However, the Cu present a melting point temperature lower than for Be and Ti.
The maximum energy deposition is produced in the Cu bulk of the spoiler (see Fig. 15). The instantaneous temperature rise along the spoiler is shown in Fig 16. In this case, the maximum increment of temperature in the spoiler is of about 2500 K, clearly superior than both the fracture limit ($\Delta T_{\mathrm{fr}} \simeq 201$ K) and the melting limit ($\Delta T_{\mathrm{melt}} \simeq 1065$ K).

# 6 Conclusions

The energy collimation system of the Compact Linear Collider (CLIC) fulfils the important function of protection against mis-steered or errant beams. A spoiler and a

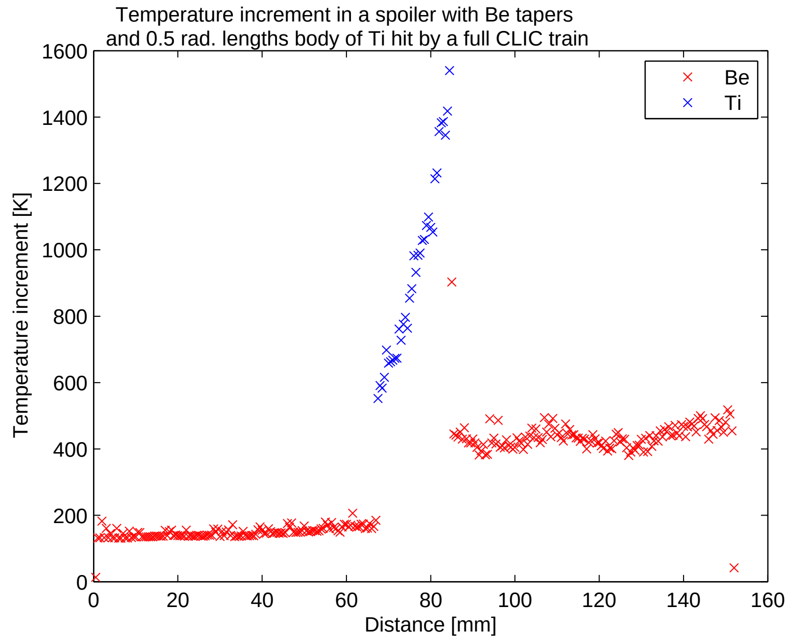


Figure 13: Instantaneous increment of temperature in a spoiler with shallow tapers of Be and $L_{\mathrm{F}} = 0.5$ $X_0$ of Ti by the impact of an entire bunch train in CLIC.

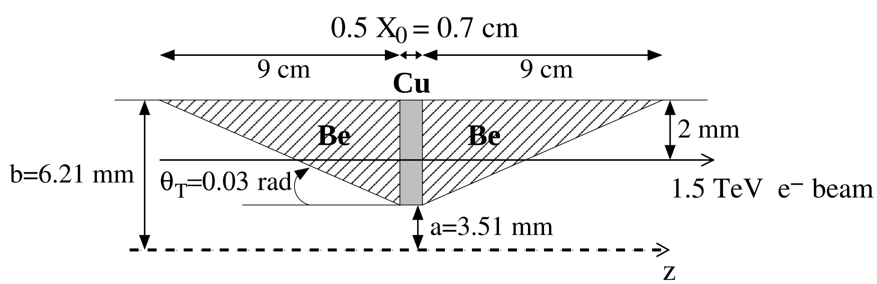


Figure 14: Schematic of the geometry used for the simulation using a Be + Cu spoiler. The figure is not to scale and the taper angle has been exaggerated.

downstream absorber in a section of the beam delivery system with non-zero horizontal dispersion are dedicated to intercept the errant beams with mean energy offsets $\gtrsim |\pm 1.5|$ % of the nominal energy peak. Here we have considered the CLIC nominal energy 1.5 TeV.

In principle, passive protection has been required for the momentum collimators. The momentum spoiler was designed with the condition of surviving in case of a deep impact of the entire bunch train. Earlier studies of the CLIC spoiler heating and spoiler damage limit [1] concluded that a spoiler made of beryllium might be a suitable solution in terms of a high robustness and acceptable wakefields. In these earlier studies no geometry for the spoiler was exactly defined.

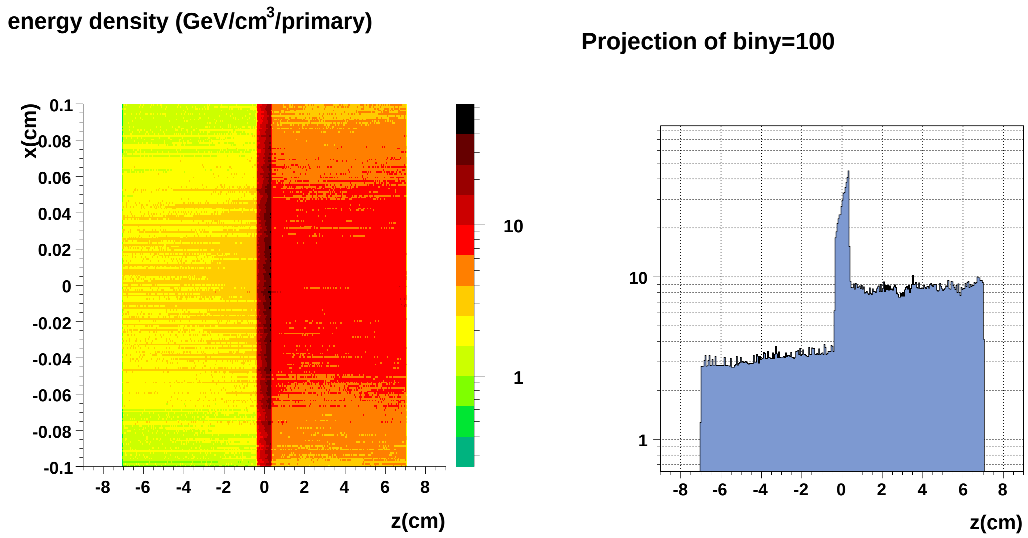


Figure 15: Density of energy deposited by ionization in the Be + Cu spoiler due to the impact of a 1.5 TeV $e^-$ beam. Right: projection of the energy density on the longitudinal coordinate $z$ for the slice $x = 0$ cm.

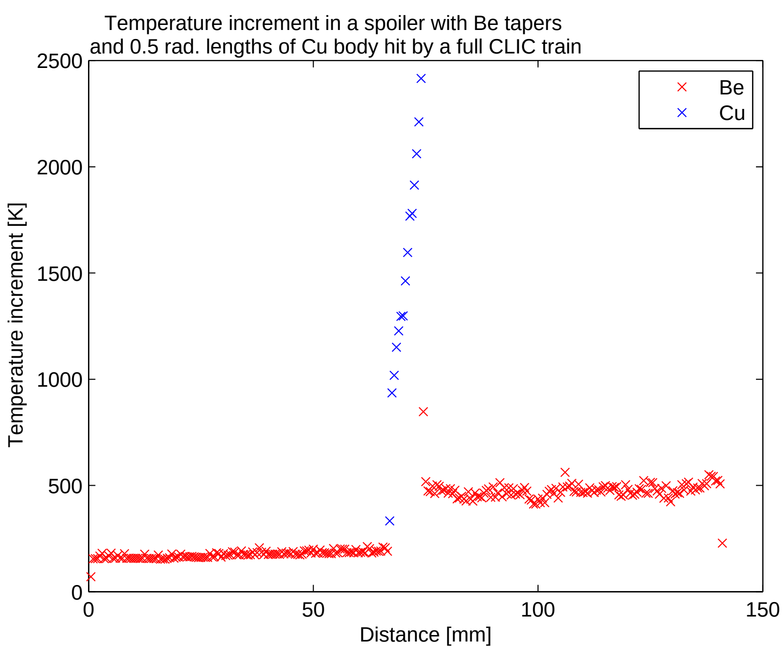


Figure 16: Instantaneous increment of temperature in a spoiler with shallow tapers of Be and $L_{\mathrm{F}} = 0.5\ \mathrm{X}_0$ of Cu by the impact of an entire bunch train in CLIC.

Since, in order to optimise the CLIC performance, the CLIC beam parameters are subject to a continue review and update [2, 3], we have revisited the CLIC energy spoiler survival issue. In this report, after defining the geometrical features of the CLIC energy spoiler, we have calculated the temperature increment in the spoiler due to instantaneous heat deposition by a full train which deeply impact on the spoiler. These calculations have been performed using the FLUKA Monte Carlo code [4] and the most recent CLIC beam parameters [3]. The FLUKA simulations have shown that a Be spoiler, such as defined in this paper, could survive the impact of the entire train.
We have also investigated other two different options: a spoiler combining Be (tapers) and Ti alloy (central body of 0.5 $X_0$), and another spoiler combining Be (tapers) and Cu (central body of 0.5 $X_0$). Since Ti and Cu present lower radiation length than Be, these options could help to increase the angle divergence of the errant beam at the downstream absorber, guaranteeing thus the passive protection of the absorber. Table 6 summarises the results. According to these results, the increment of temperature in the Be (tapers) + Ti alloy spoiler remains slightly below both the thermal fracture limit and the melting limit. Therefore, a spoiler structure combining Be and Ti alloy might be another possible solution in terms of robustness. On the other hand, for the Be + Cu spoiler the increment of temperature is largely higher than both the thermal fracture and the melting points. Nevertheless, it is necessary to point out that for these simulations we have assumed monochromatic beams (no energy spread), which gives higher beam energy densities than assuming a certain energy spread. Therefore, the results of Table 6 give an upper limit and can be considered as pessimistic. The situation would be more favourable for spoiler survival if a realistic CLIC-like beam distribution is considered (using an uniform energy spectrum with a 1 % full width energy spread).

Table 6: Instantaneous temperature rise ($\Delta\hat{T}_{inst}$) and the cyclic thermal stress ($\sigma_{cyc}$) calculated using the code FLUKA for the three options of energy spoiler studied in this report. The result is compared with the thermal fracture temperature increment limit ($\Delta T_{\mathrm{fr}}$) and the melting temperature increment limit ($\Delta T_{\mathrm{melt}}$).

| **Variable** | Be | Ti alloy (0.5 $X_0$ flat part) | Cu (0.5 $X_0$ flat part) |
|---|---|---|---|
| $\Delta\hat{T}_{inst}$ [K] (FLUKA) | 280 | 1600 | 2500 |
| $\sigma_{cyc}$ [MPa] (FLUKA) | 454 | 944 | 2681 |
| $\Delta T_{\mathrm{melt}}$ [K] | 1267 | 1648 | 1065 |
| $\Delta T_{\mathrm{fr}}$ [K] | 370 | 1710 | 201 |

Finally we can conclude that a Be based spoiler could survive the impact of the entire CLIC bunch train and would provide a suitable solution for the CLIC energy collimation system. Nevertheless, an important inconvenience of using Be is that the manipulation of the Be presents technical challenges due to its toxicity (especially by inhalation) of Be-containing dusts. Although challenging, the Be spoiler is a solution relatively simpler in comparison with other proposals, e.g. rotating consumable collimators [18].

## Acknowledgements

The authors wish to thank Dr. Daniel Schulte and Dr. Frank Zimmermann for the review of this manuscript, and Dr. Rogelio Tomás for many helpful discussions.
This work is supported by the Commission of the European Communities under the $6^{th}$ Framework Programme "Structuring the European Research Area", contract number RIDS-011899.

## References

[1] S. Fartoukh, J. B. Jeanneret and J. Pancin, "Heat deposition by transient beam passage in spoilers", CERN-SL-2001-012 AP, CLIC Note 477, 2001.

[2] F. Tecker, *et al.*, "Updated CLIC Parameters 2005", CLIC Note 627 (2006), CERN-OPEN-2006-022 (2006).

[3] F. Tecker, *et al.*, CLIC Draft Parameter List, http://clic-meeting.web.cern.ch/clic-meeting/clictable2007.html.

[4] A. Fasso, *et al.*, "FLUKA: a multi-particle transport code", CERN-2005-10 (2005), INFN/TC-05/11, SLAC-R-773.

[5] P. Raimondi and A. Seyi, "Novel Final Focus Design for Future Linear Colliders", Phys. Rev. Lett. **86** (2000) 3779.

[6] R. Tomás, "Optimizing the CLIC Beam Delivery System", CERN-OPEN-2008-008; CLIC-Note-735, 2008.

[7] D. Schulte and F. Zimmermann, "Failure Modes in CLIC", PAC2001, Chicago, USA, 2001; CLIC Note 492 (2001); CERN-SL-2001-034 (AP) (2001).

[8] R. Assmann *et al.*, "Collimation for CLIC", CERN-AB-2003-075 (2003).

[9] R. Tomás, private communication (June, 2008).

[10] H. Grote and F. C. Iselin, "The MAD Program, User's Reference Manual", CERN-SL-90-13 (AP) (1996); see the web site: http://mad.home.cern.ch/mad.

[11] D. Schulte *et al.*, "Simulation Package based on PLACET", PAC2001, Chicago, USA, 2001; CLIC Note 482 (2001); CERN/PS 2001-028 (AE) (2001), see the web site: https://savannah.cern.ch/projects/placet.

[12] Particle Data Group, Journal of Physics G **33** (2006) 1.

[13] David R. Lide (ed), "CRC Handbook of Chemistry and Physics", 84th Edition, CRC Press. Boca Raton, Florida, 2003.

[14] A. M. James and M. P. Lord, “Macmillan’s Chemical and Physical Data”, Macmillan, London, UK, 1992.

[15] G. W. C. Kaye and T. H. Laby, “Tables of physical and chemical constants”, Longman, London, UK, 15th edition, 1993.

[16] A. M. Howatson, P. G. Lund and J. D. Todd, “Engineering Tables and Data”, Chapman & Hall, London, 1991.

[17] L. Fernández-Hernando, and N. K. Watson, “FLUKA simulations of energy density deposition from a ILC bunch in different spoiler designs”, EUROTeV-Report-2006-015, March 2006.

[18] J. Frisch, E. Doyle, K. Skarpaas, “Advanced Collimator Prototype Results for the NLC.”, SLAC-PUB-8463 (2000).